Published OnlineFirst on January 11, 2011; DOI:10.1158/0008-5472.CAN-10-2842

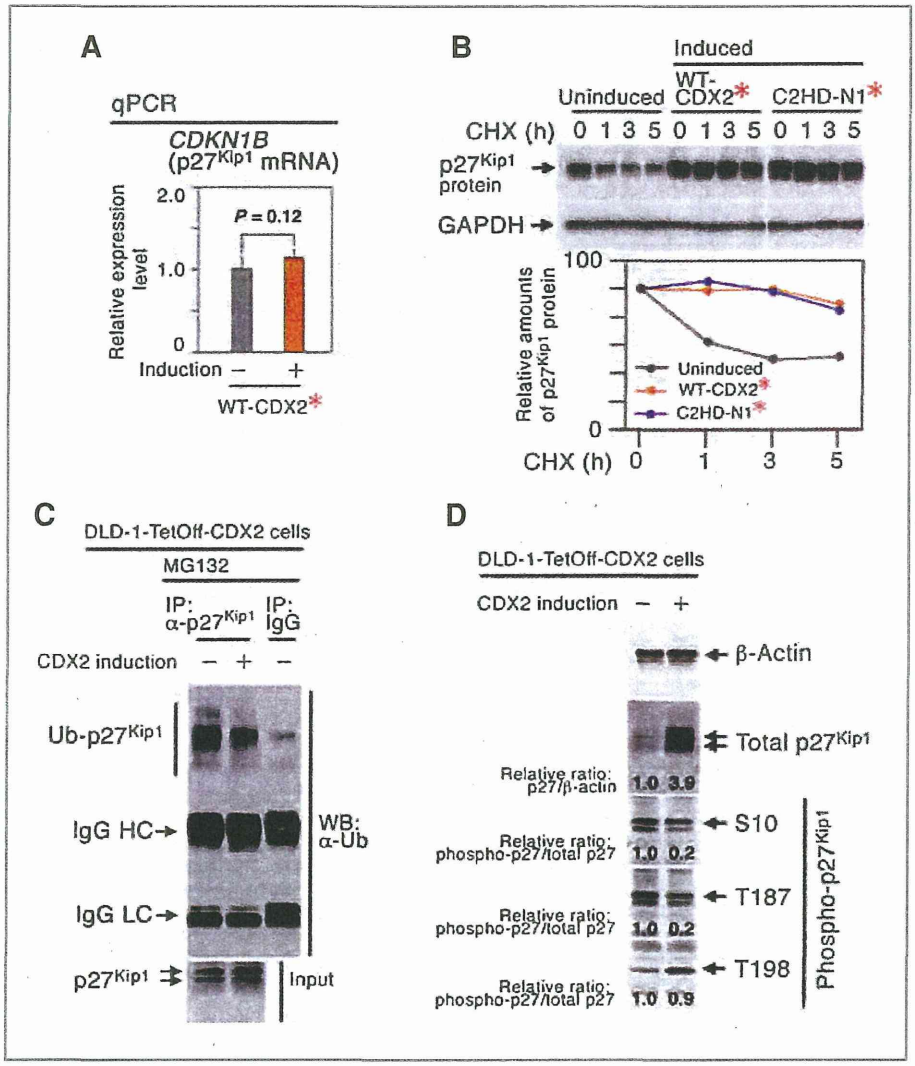

Figure 4. CDX2 stabilizes $p27^{Kip1}$ protein by blocking its ubiquitylation. A, amount of $p27^{Kip1}$ (*CDKN1B*) mRNA on day 2 of induction of wild-type CDX2 in DLD-1–TetOff cell clones, analyzed by quantitative PCR (qPCR). B, amount of $p27^{Kip1}$ protein at the indicated hours after treatment with cycloheximide (CHX) on induction of wild-type CDX2 or C2HD-N1 protein, analyzed by Western blotting (top). GAPDH was used as a loading control. Quantified data are shown in bottom. C, the level of polyubiquitylated $p27^{Kip1}$, analyzed by Western blotting, on expression of CDX2 in DLD-1 cells. DLD-1–TetOff cells were treated with 10 μmol/L of MG132 for 12 hours to inhibit proteasome activity. $p27^{Kip1}$ in the cell lysate was immunoprecipitated using an antibody for $p27^{Kip1}$, and the level of polyubiquitylated $p27^{Kip1}$ was analyzed by Western blotting, using an antibody for ubiquitin. D, phosphorylation levels of $p27^{Kip1}$ at S10, T187, and T189 analyzed by Western blotting, on expression of CDX2 in DLD-1–TetOff cells. β-Actin was used as a loading control. Numbers for S10, T187, and T189 phosphorylation indicate relative ratios of the phosphorylated $p27^{Kip1}$ to the total $p27^{Kip1}$, whereas those for total $p27^{Kip1}$ indicate relative levels of $p27^{Kip1}$ to β-actin.

and *HEPH* genes (Supplementary Fig. S1A), both controlled by CDX2 (18, 19). Importantly, induction of CDX2 arrested the TetOff cells in the G0/G1 cell-cycle phase and suppressed proliferation (Fig. 1D, right; Supplementary Figs. S1B and S2A). The same results were obtained with mouse colon cancer cells Colon26, in which Wnt signaling was not activated (Supplementary Fig. S1C and D). Consistently, knockdown of endogenous CDX2 expression increased the S-phase fraction by approximately 10% (Supplementary Fig. S2B and C). These results suggest that CDX2 suppresses proliferation of not only normal and adenoma epithelia but also colon cancer cells by blocking G0/G1-S progression.

Nontranscriptional activity of CDX2 in N-terminal and homeobox domains is sufficient to block cell proliferation

Because homeobox proteins function as transcription factors through their HDs (20), we investigated whether CDX2 blocked cell proliferation through its transcriptional activity. To this end, we constructed transcription-defective CDX2 mutants that contained point mutations in the HD (Fig. 2A, left). Mutations R189A, R237A, R237H, and R237P have been reported to eliminate the binding activity of HD to DNA, whereas Q234K alters its DNA-binding specificity (21). These HD mutations (R189A, Q234K, R237A, R237H, and R237P) lost the transcriptional activation for CDX2-target gene promoters (Fig. 2A, left, *LI-cadherin* gene promoter; Supplementary Fig. S3A, *HEPH* promoter), although all mutant proteins were stable, and localized predominantly to the nucleus (Supplementary Fig. S4A and B). Consistently, the HD mutations lost DNA-binding activity for the CDX2-target gene promoters (Fig. 2A, right, *LI-cadherin* gene promoter; Supplementary Fig. S3B, *sucrase isomaltase* promoter). Surprisingly, the transcription-defective CDX2 mutants (R189A, Q234K, R237A, and R237H) retained similar blocking activities on cell proliferation to that of the wild type (WT; Fig. 2B; Supplementary

Published OnlineFirst on January 11, 2011; DOI:10.1158/0008-5472.CAN-10-2842

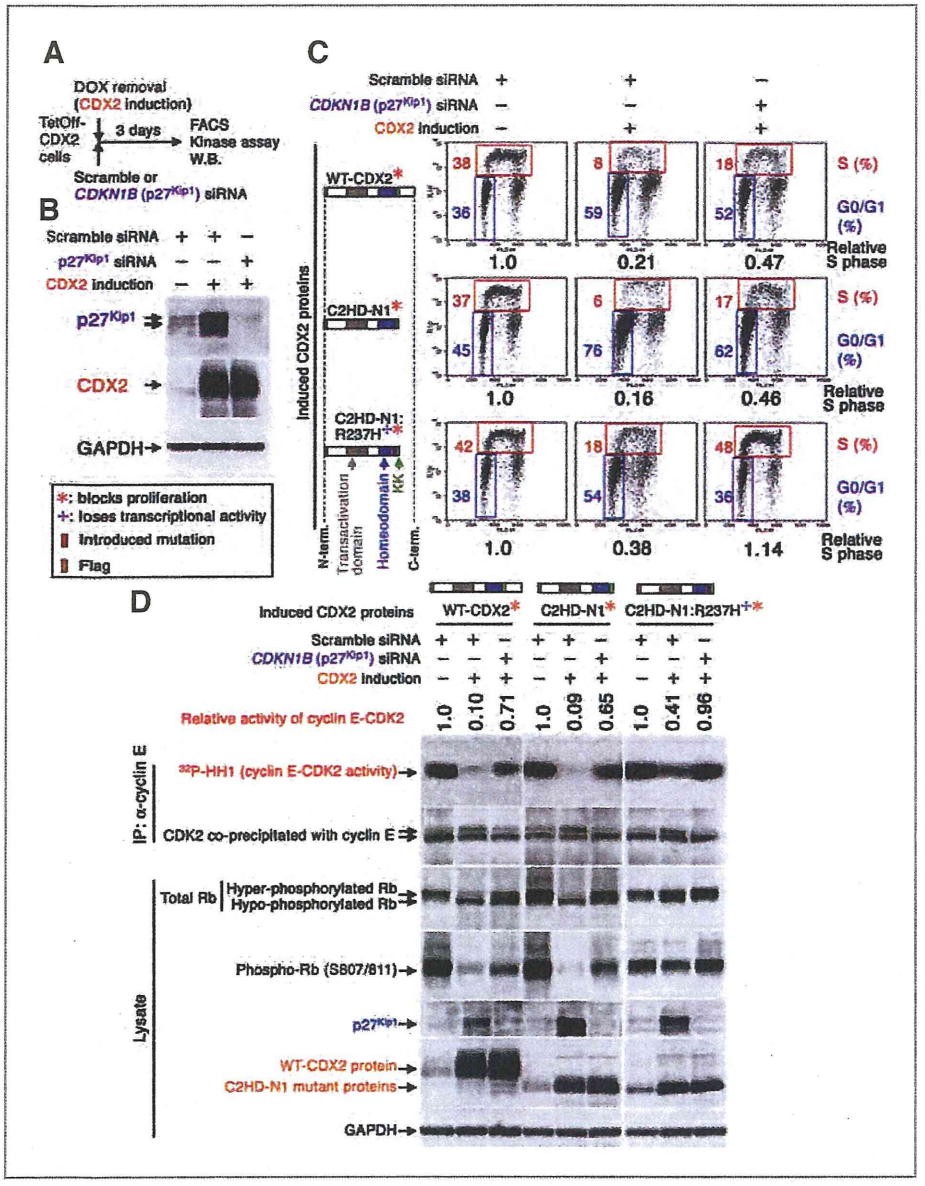

Figure 5. $p27^{Kip1}$ is critical for CDX2 to block cell-cycle progression. A and B, suppression of $p27^{Kip1}$ expression on day 3 after introduction of *CDKN1B* ($p27^{Kip1}$) siRNA simultaneously with expression of wild-type CDX2 in TetOff cells (A; schematic experimental strategy), analyzed by Western blotting (B, top). Band for CDX2 is also shown in the middle (B). GAPDH was used as a loading control (B, bottom). C, cell-cycle profiles on day 3 after introduction of $p27^{Kip1}$ siRNA and simultaneous expression of wild-type CDX2 (top), mutant C2HD-N1 (middle), or transcription-defective mutant C2HD-N1:R237H (bottom) in TetOff cells, analyzed by flow cytometry. D, kinase activity of cyclin E-CDK2 (IP; anti-cyclin E) on histone H1 (HH1) substrate on day 3 after introduction of $p27^{Kip1}$ siRNA and simultaneous expression of WT-CDX2 (left), C2HD-N1 (center), or C2HD-N1: R237H (right) in TetOff cells, analyzed by *in vitro* kinase assay. Incorporation of ^{32}P into HH1 is shown (top). The level of CDK2 coimmunoprecipiated with cyclin E was also analyzed by Western blotting. The relative kinase activities of cyclin E-CDK2 are shown above the photo. Phosphorylation level of Rb in the TetOff cell lysate on day 3 was also analyzed by Western blotting.

Fig. S3C). Importantly, these results suggest that both transcriptional and DNA-binding activities are dispensable for blocking proliferation by CDX2. On the contrary, another mutation R237P suppressed inhibition of cell proliferation by CDX2 (Fig. 2B), suggesting that HD was essential for the block of proliferation.

To localize in CDX2 the domains responsible for blocking cell proliferation, we then constructed deletion mutants "C2HDs" that retained its HD (Fig. 2C). Mutant C2HD-KK contained HD and its C-terminally adjacent lysyl-lysine (KK; Fig. 2C). Mutants C2HD-N1 and -N4 contained HD with C-terminal KK, and N-terminal extensions (Fig. 2C). Because mutant C2HD-N1 retained the transactivation domain (22) and activated the *LI-cadherin* and *HEPH* promoters, we also constructed its transcription-defective derivatives that carried HD mutations R237A and R237H (C2HD-N1:R237A and -N1: R237H, respectively; Fig. 2C). All C2HD proteins were expressed stably in DLD-1 cells (Supplementary Fig. S5A and B), whereas we failed to construct cells expressing CDX2 deletion mutant proteins lacking HD, due to their instability *in vivo* (data not shown). Like WT-CDX2 and C2HD-N1, cell proliferation was still blocked by induction of C2HD-N1 derivatives that lacked both the C-terminal domain and transcriptional activity (C2HD-N1:R237A and -N1:R237H; Fig. 2C and D; Supplementary Fig. S6A and B). These results indicate that CDX2 C-terminal domain as well as

Published OnlineFirst on January 11, 2011; DOI:10.1158/0008-5472.CAN-10-2842

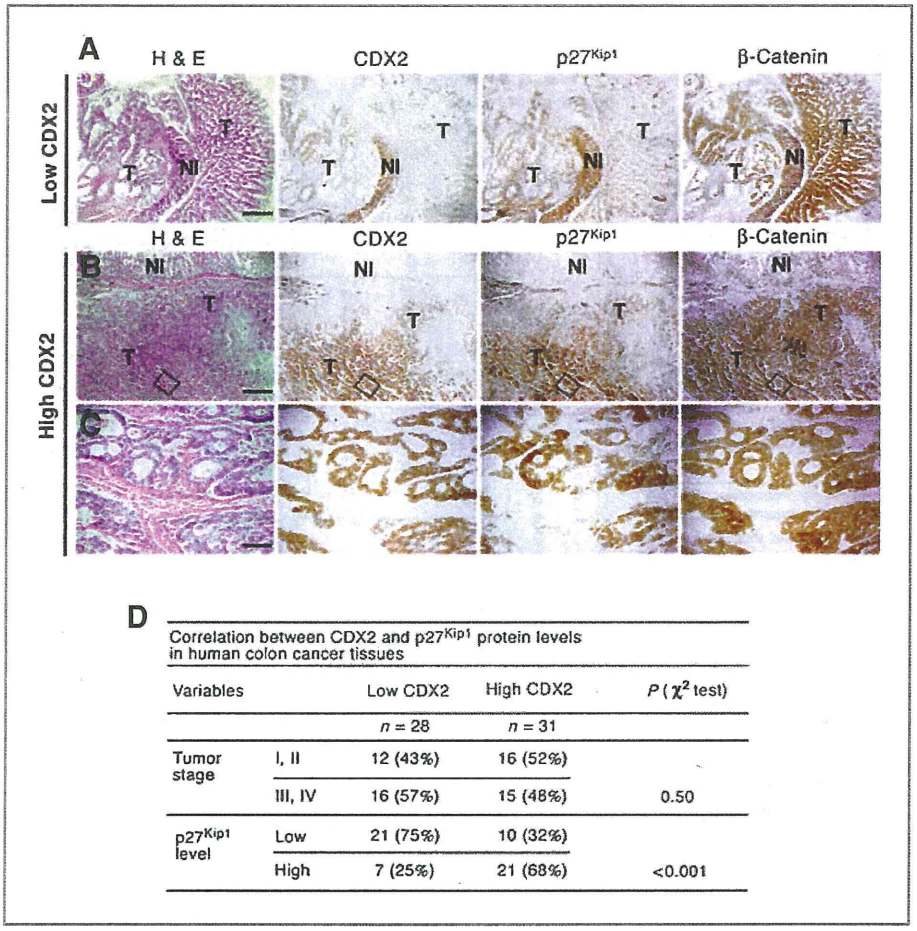

Figure 6. Correlation between CDX2 and $p27^{Kip1}$ levels in human colon cancer tissues. A–C, representative photographs for the low-CDX2 (A) and high-CDX2 (B and C) colon cancer tissues. Tissues were stained with hematoxylin and eosin, or antibodies for CDX2, $p27^{Kip1}$, or β-catenin. C, higher magnifications of insets in B, respectively. T, tumor tissue; NI, normal mucosa. β-Catenin was used as a positive control for immunohistochemistry. Note that the level of β-catenin was increased in the tumor tissue compared with that in normal mucosa. Bars, 1 mm. D, correlation between the CDX2 and $p27^{Kip1}$ levels in 59 human colon cancer specimens. P values were obtained by the $\chi 2$ test.

D

Correlation between CDX2 and $p27^{Kip1}$ protein levels in human colon cancer tissues

Variables		Low CDX2	High CDX2	P (χ^2 test)
		$n = 28$	$n = 31$	
Tumor stage	I, II	12 (43%)	16 (52%)	
	III, IV	16 (57%)	15 (48%)	0.50
$p27^{Kip1}$ level	Low	21 (75%)	10 (32%)	
	High	7 (25%)	21 (68%)	<0.001

transcriptional activity was dispensable for the proliferation block. Although cell proliferation was also blocked by C2HD-KK and C2HD-N4 (Fig. 2D), the effect was only partial, suggesting that the HD alone was insufficient, and its N-terminal domain was needed for the full activity of CDX2.

CDX2 increases amounts of $p27^{Kip1}$ protein and cyclin-CDK2/$p27^{Kip1}$ complex

Progression from the G1 to S phase is positively regulated by the cyclin E-CDK2 complex (23). We found that the cellular cyclin E-CDK2 kinase activity was decreased by expression of WT-CDX2 or its mutants (CDX2:R237A and C2HD-N1), as assayed by histone H1 (HH1) phosphorylation (Fig. 3A; total CDK2 activity, Supplementary Fig. S7A, left). At the same time, induction of WT-CDX2 or mutant CDX2:R237A increased the amounts of cyclin E, cyclin A, and CDK2 coimmunoprecipitated with $p27^{Kip1}$, whereas the induction reduced the lysate levels of cyclin A and CDK2 (Fig. 3B). Induction of WT-CDX2 or CDX2:R237A also increased the level of total $p27^{Kip1}$ protein in the lysate of DLD-1 cells (Fig. 3C, left; for quantified data, Supplementary Fig. S7A, right, by approximately 3 times), without affecting the subcellular localizations of the cyclins, CDK2 and $p27^{Kip1}$ (Supplementary Fig. S7B, left). Also, in LS174T cells, the level of $p27^{Kip1}$ was increased on expression of CDX2 (Fig. 3C, right). These results suggest that expression of CDX2 increases the amounts of cyclin E-CDK2/$p27^{Kip1}$ and cyclin A-CDK2/$p27^{Kip1}$ complexes through raising the level of $p27^{Kip1}$. Consistently, the $p27^{Kip1}$ protein level was decreased in the reduced-CDX2 cells (by approximately 40%; Fig. 3D, left) and *Cdx2*$^{+/-}$ colonic hamartomas where CDX2 was essentially absent (by approximately 90%; Fig. 3D, right).

Also, by expression of deletion mutant C2HD-N1 and its transcription-deficient derivatives (C2HD-N1:R237H and -N1:R237A), the level of $p27^{Kip1}$ in cell lysates was increased, as well as those of cyclin E- and cyclin A-CDK2/$p27^{Kip1}$ complexes (Fig. 3B and C; Supplementary Fig. S7B, right). On the contrary, mutation R237P suppressed increase in the level of $p27^{Kip1}$ (Supplementary Fig. S7C). These results show that the N-terminal and HD in CDX2 are sufficient for increasing the $p27^{Kip1}$ level and blocking proliferation.

Expression of CDX2 stabilizes $p27^{Kip1}$ by blocking its ubiquitylation

In contrast to the increased level of $p27^{Kip1}$ protein (Fig. 3C), its mRNA (*CDKN1B*) level remained unchanged on induction of CDX2 (Fig. 4A), suggesting that CDX2 stabilized $p27^{Kip1}$

Published OnlineFirst on January 11, 2011; DOI:10.1158/0008-5472.CAN-10-2842

protein. To test this possibility, we treated CDX2-induced cells with CHX, an inhibitor of protein translation. In the CDX2-uninduced control cells, the level of $p27^{Kip1}$ protein decreased by approximately 50% in 3 hours after CHX treatment (Fig. 4B). However, the level decreased only by approximately 10% on induction of WT-CDX2 or C2HD-N1 protein (Fig. 4B), showing that CDX2 stabilized $p27^{Kip1}$ protein.

Stability of $p27^{Kip1}$ is controlled by SKP2 through ubiquitylation-mediated proteolysis (24–29). Because polyubiquitylated $p27^{Kip1}$ is detectable when its proteasomal degradation is inhibited, we treated CDX2-induced cells with MG132, a proteasome inhibitor. Notably, the level of polyubiquitylated $p27^{Kip1}$ was decreased on expression of CDX2 (Fig. 4C), whereas those of polyubiquitylated cyclins E and A, other SKP2 targets, were increased (Supplementary Fig. S7D). Because these results suggested that the $p27^{Kip1}$ ubiquitylation was specifically suppressed by CDX2 expression, we further investigated the $p27^{Kip1}$ phosphorylation that can control its ubiquitylation (24–31). The ratios of S10- and T187-phosphorylated $p27^{Kip1}$ to the total $p27^{Kip1}$ were reduced significantly to approximately 20% on induction of CDX2, whereas that of T198 was not affected (Fig. 4D). The phosphorylation of $p27^{Kip1}$ at T187 reduces the stability of $p27^{Kip1}$ through accelerating the ubiquitylation-mediated degradation, whereas that of S10 stabilizes $p27^{Kip1}$ (30–33). Thus, it is likely that the reduced level of the T187 phosphorylation is a main cause of the $p27^{Kip1}$ stabilization on expression of CDX2.

$p27^{Kip1}$ is critical for CDX2 to block cell-cycle progression

To investigate further the role of $p27^{Kip1}$ in the CDX2-mediated proliferation block, we simultaneously induced CDX2, and suppressed $p27^{Kip1}$ expression by introducing siRNA against *CDKN1B* ($p27^{Kip1}$ siRNA) into the TetOff–CDX2 cells (Fig. 5A and B). Notably, knocking down $p27^{Kip1}$ completely prevented the decrease in the S-phase fraction on expression of C2HD-N1:R237H (transcription-defective C2HD-N1 mutant; Fig. 5C, bottom; compare center and right). These results show that the increased level of $p27^{Kip1}$ is essential for CDX2 to block G0/G1-S phase progression. Consistently, reducing the level of $p27^{Kip1}$ completely blocked the decrease in the cyclin E–associated CDK2 activity on expression of C2HD-N1:R237H (Fig. 5D; right, top) or C2HD-N1:R237A (Supplementary Fig. S8). The reduced level of $p27^{Kip1}$ in C2HD-N1:R237H–induced cells also blocked the decrease in the phosphorylation level of retinoblastoma protein (Rb; Fig. 5D, right), an endogenous target by cyclin E-CDK2 (34, 35). These results collectively indicate that CDX2 stabilizes $p27^{Kip1}$ through its nontranscriptional activity, which causes inhibition of cyclin E-CDK2 and blocks cell proliferation.

Furthermore, reducing the level of $p27^{Kip1}$ partially suppressed the decrease in the S-phase fraction on expression of WT-CDX2 or C2HD-N1 that retained transcriptional activity (Fig. 5C, top and middle). Consistently, the reduced level of $p27^{Kip1}$ partially suppressed the decreases in cyclin E-CDK2 activity and phosphorylation level of Rb (Fig. 5D, left and center). These results verify that $p27^{Kip1}$ is critical for CDX2 to block cell-cycle progression and suppress the cyclin E-CDK2 activity, although the transcriptional activity of CDX2 may also make some contribution to the cell-proliferation block.

Correlation between CDX2 and $p27^{Kip1}$ levels in human colon cancer tissues

Finally, we analyzed expression of CDX2 and $p27^{Kip1}$ proteins in 59 human colon cancer specimens, and investigated possible correlation between their levels. Among these tumors, 28 showed the lower level of CDX2 protein compared with that in normal mucosa (Nl; Fig. 6A and 6D), whereas the other 31 showed CDX2 at similar to those at higher levels (Fig. 6B–D). Notably, the $p27^{Kip1}$ level was reduced in 21 of the 28 low-CDX2 tumors (75%; Fig. 6A and D; Supplementary Fig. S9), whereas it was reduced in only 10 of the 31 high-CDX2 tumors (Fig. 6B–D, 32%; $P < 0.001$, obtained from χ^2 test). These data are consistent with the results that the $p27^{Kip1}$ level was reduced in the low-CDX2 colon cancer cell lines and $Cdx2^{+/-}$ mutant mouse colonic tumors (Fig. 3D). Collectively, these results suggest that low levels of CDX2 contribute to the reduced levels of $p27^{Kip1}$ in human colon cancer tissues. On the contrary, $p27^{Kip1}$ protein in 21 of the 31 high-CDX2 tumors (68%; Fig. 6B–D; Supplementary Fig. S10), whereas it was retained in only 7 of the 28 low-CDX2 tumors (25%; Fig. 6D). These data are also consistent with the results that CDX2 increased the level of $p27^{Kip1}$ protein in colon cancer TetOff cells (Fig. 3C), showing a positive correlation between CDX2 and $p27^{Kip1}$ levels.

Discussion

In human cancer cells of the colon and other epithelial tissues, the level of $p27^{Kip1}$ is frequently reduced by its accelerated degradation through proteasomes (36, 37). The reduced level of $p27^{Kip1}$ is also correlated with poor prognosis, suggesting its tumor-suppressing activity (25). Consistently, homozygous $p27^{Kip1}$ mutation increased the number of intestinal polyps in *Apc* mutant mice by 5 to 6 times (38). In colon cancer cells, however, the mechanism that stimulates the degradation of $p27^{Kip1}$ was unknown. Here we have shown that homeobox transcription factor CDX2 stabilizes $p27^{Kip1}$ by blocking its proteolysis (Figs. 3 and 4). Interestingly, we have found a significant correlation between CDX2 and $p27^{Kip1}$ protein levels in human colon cancer tissues (Fig. 6). Our present results suggest that the decreased level of CDX2 is one of the causes that stimulate the $p27^{Kip1}$ proteolysis in colon cancer cells.

During the G1 to S transition, phosphorylation of $p27^{Kip1}$ at T187 triggers its proteasomal degradation through the SCF-SKP2 E3 ubiquitin ligase complex (24, 26–29). The levels of SKP2 and Cks1 were not affected by expression of CDX2:R237A that increased $p27^{Kip1}$ (Fig. 3C, left), suggesting that CDX2 stabilizes $p27^{Kip1}$ protein independent of SKP2 and Cks1 levels. Notably, the extent of $p27^{Kip1}$ phosphorylation at T187 decreased on expression of CDX2 (Fig. 4D), suggesting that CDX2 suppressed the SKP2-dependent proteolysis of $p27^{Kip1}$, which caused $p27^{Kip1}$ accumulation (Fig. 3C). Consistently, the level of $p27^{Kip1}$ ubiquitylation was reduced on expression of CDX2 (Fig. 4C). On the contrary, the reduced activity of cyclin

Published OnlineFirst on January 11, 2011; DOI:10.1158/0008-5472.CAN-10-2842

E-CDK2 can stabilize $p27^{Kip1}$ because cyclin E-CDK2 phosphorylates $p27^{Kip1}$ at T187 and accelerates its proteasomal degradation (24, 26–29). Importantly, reducing the level of $p27^{Kip1}$ blocked decreases in the cyclin E-CDK2 activity and S-phase fraction caused by CDX2 (Fig. 5C and Fig. 5D). These results indicate that $p27^{Kip1}$ is a critical downstream target of CDX2 in regulating the cyclin E-CDK2 activity and blocking cell-cycle progression. Thus, $p27^{Kip1}$ stabilization may precede the attenuated activity of cyclin E-CDK2 in CDX2-induced cells (Fig. 3A and C). It remains to be investigated how CDX2 reduces the level of $p27^{Kip1}$ phosphorylation at T187.

The level of $p27^{Kip1}$ phosphorylation at S10 was also decreased on expression of CDX2 (Fig. 4D). Because the S10 dephosphorylation promotes binding of $p27^{Kip1}$ to cyclin-CDK complex, it helps $p27^{Kip1}$ to inhibit the cyclin-CDK activity and suppress tumor development (30, 31). Thus, it is conceivable that the reduced $p27^{Kip1}$ phosphorylation at S10 also contributes to the tumor-suppressive function of CDX2.

Interestingly, knocking down $p27^{Kip1}$ completely blocked the decreases in the cyclin E-CDK2 activity and S-phase fraction on expression of the mutant C2HD-N1:R237H or C2HD-N1:R237A that lacked transcriptional activity and C-terminal domain of CDX2 (Fig. 5C and D; Supplementary Fig. S8). These results show that CDX2 stabilizes $p27^{Kip1}$ through the nontranscriptional function mediated by its N-terminal and homeobox domains. The results have also prompted us to question whether the transcription-independent function of CDX2 is shared among the CDX family proteins. To address this issue, we constructed DLD-1–TetOff cells that expressed CDX1 (Supplementary Fig. S11A), the closest homolog of CDX2. The CDXs show a high similarity in their HDs (aa identity, 92%; and similarity, 97%: Supplementary Fig. S12A), but only low similarities in both N-terminal and C-terminal domains (aa similarities, 42% and 38%, respectively: Supplementary Fig. S12B and C). Expression of CDX1 did not increase the $p27^{Kip1}$ level in the DLD-1 cells (Supplementary Fig. S11C), although the level of induced CDX1 and its transcriptional activity were comparable to those of CDX2 (Supplementary Fig. S11A and B). Thus, it appears that the transcription-independent block of proliferation is specific to CDX2. Because the HDs are almost identical between the CDXs (Supplementary Fig. S12A), the N-terminal domain can be critical for the nontranscriptional function of CDX2. This interpretation is consistent with the results that C2HD-N1 (N-terminal and HD) increases the level of $p27^{Kip1}$ protein by approximately 5 times, whereas C2HD-KK alone does it only by approximately 1.5 times (Fig. 3C, left; Supplementary Fig. S7A, center). To understand the precise role of the N-terminal domain of CDX2 in stabilizing $p27^{Kip1}$, it will be interesting to identify proteins that can bind to the domain.

Wnt, Notch, and PI3K-Akt signaling pathways are proposed as major mechanisms that stimulate proliferation of the colonic epithelial cells (16, 39, 40). On the contrary, the $Cdx2^{+/-}$ mutation stimulated proliferation of the $Apc^{-/-}$ adenoma epithelial cells in which Wnt and Notch signaling pathways were already activated (Fig. 1C; refs. 16, 39, 40). Expression of CDX2 also blocked the proliferation of colon cancer cells in which the Wnt and PI3K signaling pathways were activated through mutations in the *APC*, β-catenin, or *PIK3CA* gene (Fig. 1D; refs. 16, 17). Collectively, these results may indicate that CDX2 functions as an additional layer of regulation that inhibits proliferation of the colonic epithelial cells, and ensures a quick halt of the cell cycle as soon as the transit-amplifying cells initiate differentiation.

Disclosure of Potential Conflicts of Interest

No potential conflicts of interest disclosed.

Acknowledgments

We thank M. Maekawa for technical assistance and Dr. A. Shimizu for the flow cytometry service. We also thank Drs. G. Baldassarre, M. Schiappacassi, T. Yamashita, and M. Sonoshita for fruitful discussion, and Drs. K. Ookawa and M. Sugai for technical advice. We thank Dr. Y. Tamai for *Cdx2* mutant mice.

Grant Support

This work was supported by grants-in-aid for scientific research (to M. M. Taketo) and for young scientist B (to K. Aoki) from the Ministry of Education, Culture, Sports, Science, and Technology, Japan.

The costs of publication of this article were defrayed in part by the payment of page charges. This article must therefore be hereby marked *advertisement* in accordance with 18 U.S.C. Section 1734 solely to indicate this fact.

Received August 4, 2010; revised October 4, 2010; accepted October 4, 2010; published OnlineFirst January 11, 2011.

References

1. James R, Kazenwadel J. Homeobox gene expression in the intestinal epithelium of adult mice. J Biol Chem 1991;266:3246–51.
2. Macdonald PM, Struhl G. A molecular gradient in early Drosophila embryos and its role in specifying the body pattern. Nature 1986;324:537–45.
3. Niwa H, Toyooka Y, Shimosato D, Strumpf D, Takahashi K, Yagi R, et al. Interaction between Oct3/4 and Cdx2 determines trophectoderm differentiation. Cell 2005;123:917–29.
4. Chawengsaksophak K, James R, Hammond VE, Kontgen F, Beck F. Homeosis and intestinal tumours in *Cdx2* mutant mice. Nature 1997;386:84–7.
5. Tamai Y, Nakajima R, Ishikawa T, Takaku K, Seldin MF, Taketo MM. Colonic hamartoma development by anomalous duplication in *Cdx2* knockout mice. Cancer Res 1999;59: 2965–70.
6. Silberg DG, Swain GP, Suh ER, Traber PG. Cdx1 and cdx2 expression during intestinal development. Gastroenterology 2000;119:61–971.
7. Guo RJ, Suh ER, Lynch JP. The role of Cdx proteins in intestinal development and cancer. Cancer Biol Ther 2004;3:593–601.
8. Gao N, Kaestner KH. Cdx2 regulates endo-lysosomal function and epithelial cell polarity. Genes Dev 2010;24:1295–305.
9. Gao N, White P, Kaestner KH. Establishment of intestinal identity and epithelial-mesenchymal signaling by Cdx2. Dev Cell 2009;16:588–99.
10. Ee HC, Erler T, Bhathal PS, Young G. P, James R. J. Cdx-2 homeodomain protein expression in human and rat colorectal adenoma and carcinoma. Am J Pathol 1995;147:586–92.
11. Mallo GV, Rechreche H, Frigerio JM, Rocha D, Zweibaum A, Lacasa M, et al. Molecular cloning, sequencing and expression of the mRNA encoding human *Cdx1* and *Cdx2* homeobox. Down-regulation of

Published OnlineFirst on January 11, 2011; DOI:10.1158/0008-5472.CAN-10-2842

Cdx1 and *Cdx2* mRNA expression during colorectal carcinogenesis. Int J Cancer 1997;74:35–44.

12. Aoki K, Tamai Y, Horiike S, Oshima M, Taketo MM. Colonic polyposis caused by mTOR-mediated chromosomal instability in $Apc^{+/\Delta 716}Cdx2+/-$ compound mutant mice. Nat Genet 2003;35: 323–30.
13. Oshima M, Oshima H, Kitagawa K, Kobayashi M, Itakura C, Taketo M. Loss of *Apc* heterozygosity and abnormal tissue building in nascent intestinal polyps in mice carrying a truncated *Apc* gene. Proc Natl Acad Sci U S A 1995;92:4482–6.
14. Bonhomme C, Duluc I, Martin E, Chawengsaksophak K, Chenard MP, Kedinger M, et al. The *Cdx2* homeobox gene has a tumour suppressor function in the distal colon in addition to a homeotic role during gut development. Gut 2003;52:1465–71.
15. Kakizaki F, Aoki K, Miyoshi H, Carrasco N, Aoki M, Taketo MM. CDX transcription factors positively regulate expression of solute carrier family 5, member 8 in the colonic epithelium. Gastroenterology 2010;138:627–35.
16. van de Wetering M, Sancho E, Verweij C, de Lau W, Oving I, Hurlstone A, et al. The β-catenin/TCF-4 complex imposes a crypt progenitor phenotype on colorectal cancer cells. Cell 2002;111:241–50.
17. Samuels Y, Diaz LA Jr, Schmidt-Kittler O, Cummins JM, Delong L, Cheong I, et al . Mutant PIK3CA promotes cell growth and invasion of human cancer cells. Cancer Cell 2005;7:561–73.
18. Hinoi T, Lucas PC, Kuick R, Hanash S, Cho KR, Fearon ER, CDX2 regulates liver intestine-cadherin expression in normal and malignant colon epithelium and intestinal metaplasia. Gastroenterology 2002; 123:1565–77.
19. Hinoi T, Gesina G, Akyol A, Kuick R, Hanash S, Giordano TJ, et al . CDX2-regulated expression of iron transport protein hephaestin in intestinal and colonic epithelium. Gastroenterology 2005;128:946–61.
20. Gehring WJ, Qian YQ, Billeter M, Furukubo-Tokunaga K, Schier AF, Resendez-Perez D, et al. Homeodomain-DNA recognition. Cell 1994;78:211–23.
21. Chi, Y. I. Homeodomain revisited: a lesson from disease-causing mutations. Hum Genet 2005;116: 433-444.
22. Rings EH, Boudreau F, Taylor JK, Moffett J, Suh ER, Traber PG. Phosphorylation of the serine 60 residue within the Cdx2 activation domain mediates its transactivation capacity. Gastroenterology 2001;121:1437–50.
23. Sherr CJ, Roberts JM. CDK inhibitors: positive and negative regulators of G1-phase progression. Genes Dev 1999;13:1501–12.
24. Vlach J, Hennecke S, Amati B. Phosphorylation-dependent degradation of the cyclin-dependent kinase inhibitor p27. EMBO J 1997; 16:5334–44.
25. Chu IM, Hengst L, Slingerland JM. The Cdk inhibitor p27 in human cancer: prognostic potential and relevance to anticancer therapy. Nat Rev Cancer 2008;8:253–67.
26. Montagnoli A, Fiore F, Eytan E, Carrano AC, Draetta GF, Hershko A, et al. Ubiquitination of p27 is regulated by Cdk-dependent phosphorylation and trimeric complex formation. Genes Dev 1999;13: 1181–9.
27. Carrano AC, Eytan E, Hershko A, Pagano M. SKP2 is required for ubiquitin-mediated degradation of the CDK inhibitor p27. Nat Cell Biol 1999;1:193–9.
28. Nakayama KI, Hatakeyama S, Nakayama K. Regulation of the cell cycle at the G1-S transition by proteolysis of cyclin E and $p27^{Kip1}$. Biochem Biophys Res Commun 2001;282:853–60.
29. Sutterluty H, Chatelain E, Marti A, Wirbelauer C, Senften M, Muller U, et al. $p45^{SKP2}$ promotes $p27^{Kip1}$ degradation and induces S phase in quiescent cells. Nat Cell Biol 1999;1:207–14.
30. Kotake Y, Nakayama K, Ishida N, Nakayama KI. Role of serine 10 phosphorylation in p27 stabilization revealed by analysis of p27 knock-in mice harboring a serine 10 mutation. J Biol Chem 2005;280: 1095–102.
31. Besson A, Gurian-West M, Chen X, Kelly-Spratt KS, Kemp CJ, Roberts JM. A pathway in quiescent cells that controls $p27^{Kip1}$ stability, subcellular localization, and tumor suppression. Genes Dev 2006;20:47–64.
32. Kossatz U, Vervoorts J, Nickeleit I, Sundberg HA, Arthur JS, Manns MP, et al. C-terminal phosphorylation controls the stability and function of $p27^{kip1}$. EMBO J 2006;25:5159–70.
33. Liang J, Shao SH, Xu ZX, Hennessy B, Ding Z, Larrea M, et al. The energy sensing LKB1-AMPK pathway regulates p27(kip1) phosphorylation mediating the decision to enter autophagy or apoptosis. Nat Cell Biol 2007;9:218–24.
34. Berthet C, Klarmann KD, Hilton MB, Suh HC, Keller JR, Kiyokawa H, et al. Combined loss of Cdk2 and Cdk4 results in embryonic lethality and Rb hypophosphorylation. Dev Cell 2006;10:563–73.
35. Hinds PW, Mittnacht S, Dulic V, Arnold A, Reed SI, Weinberg RA. Regulation of retinoblastoma protein functions by ectopic expression of human cyclins. Cell 1992;70:993–1006.
36. Chu I, Sun J, Arnaout A, Kahn H, Hanna W, Narod S, et al. p27 phosphorylation by Src regulates inhibition of cyclin E-Cdk2. Cell 2007;128:281–94.
37. Loda M, Cukor B, Tam SW, Lavin P, Fiorentino M, Draetta GF, et al. Increased proteasome-dependent degradation of the cyclin-dependent kinase inhibitor p27 in aggressive colorectal carcinomas. Nat Med 1997;3:231–4.
38. Philipp-Staheli J, Kim KH, Payne SR, Gurley KE, Liggitt D, Longton G, et al. Pathway-specific tumor suppression. Reduction of p27 accelerates gastrointestinal tumorigenesis in *Apc* mutant mice, but not in *Smad3* mutant mice. Cancer Cell 2002;1:355–68.
39. He X C, Yin T, Grindley JC, Tian Q, Sato T, Tao WA, et al. PTEN-deficient intestinal stem cells initiate intestinal polyposis. Nat Genet 2007;39:189–98.
40. van Es J H, Jay P, Gregorieff A, van Gijn ME, Jonkheer S, Hatzis P, et al. Wnt signalling induces maturation of Paneth cells in intestinal crypts. Nat Cell Biol 2005;7:381–6.
41. Gu Y, Rosenblatt J, Morgan DO. Cell cycle regulation of CDK2 activity by phosphorylation of Thr160 and Tyr15. EMBO J 1992;11:3995–4005.
42. Ishida N, Kitagawa M, Hatakeyama S, Nakayama K. Phosphorylation at serine 10, a major phosphorylation site of p27(Kip1), increases its protein stability. J Biol Chem 2000;275:25146–54.

Cancer Cell
Article

Suppression of Colon Cancer Metastasis by Aes through Inhibition of Notch Signaling

Masahiro Sonoshita,[1,7] Masahiro Aoki,[1,7,9] Haruhiko Fuwa,[2] Koji Aoki,[1] Hisahiro Hosogi,[1,3] Yoshiharu Sakai,[3] Hiroki Hashida,[4] Arimichi Takabayashi,[4] Makoto Sasaki,[2] Sylvie Robine,[5] Kazuyuki Itoh,[6] Kiyoko Yoshioka,[6] Fumihiko Kakizaki,[1] Takanori Kitamura,[1] Masanobu Oshima,[1,8] and Makoto Mark Taketo[1,*]
[1]Department of Pharmacology, Graduate School of Medicine, Kyoto University, Kyoto 606-8501, Japan
[2]Laboratory of Biostructural Chemistry, Graduate School of Life Sciences, Tohoku University, Sendai 981-8555, Japan
[3]Department of Surgery, Graduate School of Medicine, Kyoto University, Kyoto 606-8501, Japan
[4]Department of Gastroenterological Surgery and Oncology, Kitano Hospital, Osaka 530-8480, Japan
[5]Equipe de Morphogenèse et Signalisation cellulaires, Institut Curie, 75248 Paris, France
[6]Department of Biology, Osaka Medical Center for Cancer and Cardiovascular Diseases, Osaka 537-8511, Japan
[7]These authors contributed equally to this work
[8]Present address: Division of Genetics, Center for Cancer and Stem Cell Research, Kanazawa University, Kanazawa 920-0934, Japan
[9]Division of Molecular Pathology, Aichi Cancer Center Research Institute, Nagoya 464-8681, Japan
*Correspondence: taketo@mfour.med.kyoto-u.ac.jp
DOI 10.1016/j.ccr.2010.11.008

SUMMARY

Metastasis is responsible for most cancer deaths. Here, we show that *Aes* (or *Grg5*) gene functions as an endogenous metastasis suppressor. Expression of Aes was decreased in liver metastases compared with primary colon tumors in both mice and humans. Aes inhibited Notch signaling by converting active Rbpj transcription complexes into repression complexes on insoluble nuclear matrix. In tumor cells, Notch signaling was triggered by ligands on adjoining blood vessels, and stimulated transendothelial migration. Genetic depletion of *Aes* in $Apc^{\Delta 716}$ intestinal polyposis mice caused marked tumor invasion and intravasation that were suppressed by Notch signaling inhibition. These results suggest that inhibition of Notch signaling can be a promising strategy for prevention and treatment of colon cancer metastasis.

INTRODUCTION

Most cancer patients die of metastasis. Although there have been substantial advances in our understanding of the mechanisms of cancer metastasis, efficient remedies for prevention and treatment of metastasis are still missing. The invasion-metastasis cascade consists of local invasion, intravasation, transport, extravasation, formation of micrometastases, and colonization (Fidler, 2003; Steeg, 2006). This sequence is completed only infrequently, causing metastatic inefficiency, and the least efficient of these steps appears to be colonization (Smith and Theodorescu, 2009). Spread of metastatic cancer cells via blood circulation is responsible for the majority of distant metastases, although they may travel also through the lymph ducts to nodes (Weinberg, 2007). In colorectal cancer, metastatic tropism to the liver and lungs can be explained largely by the organization of venous circulation of the intestines through portal vein to the liver, and further to the lungs through pulmonary artery.

Among endogenous colon tumor models, the widely used *Apc* (*Adenomatous polyposis coli*) mutant mice form adenomas in the small intestine, with wide multiplicities (3–300 per animal) depending on the mutational allele, although several adenomas are also found in the colon (Taketo and Edelman, 2009). Additional mutations introduced into *Apc* mutant mice can modify the tumor phenotype. For example, knocking out *Smad4* gene in the TGF-β family signaling converts the benign intestinal adenomas to very invasive adenocarcinomas (Takaku et al.,

Significance

We have found that Aes suppresses colon cancer metastasis by inhibiting Notch signaling pathway. The molecular mechanism of Notch inhibition is through transcriptional repression by sequestering Rbpj, NICD, and Maml1 to nuclear matrix. The cellular mode of metastasis suppression includes inhibition of transendothelial migration (TEM) of tumor cells, which blocks intravasation. Heterotypic interaction between cancer and host cells activates Notch signaling and promotes TEM of metastasizing cancer cells. Because TEM in metastasis is common to many solid tumors, this mechanism is important in various types of cancers. As a model for colon cancer invasion and intravasation, compound mutant mice for the *Apc* and *Aes* genes should be useful to evaluate upcoming therapeutics including Notch signaling inhibitors against colon cancer metastasis.

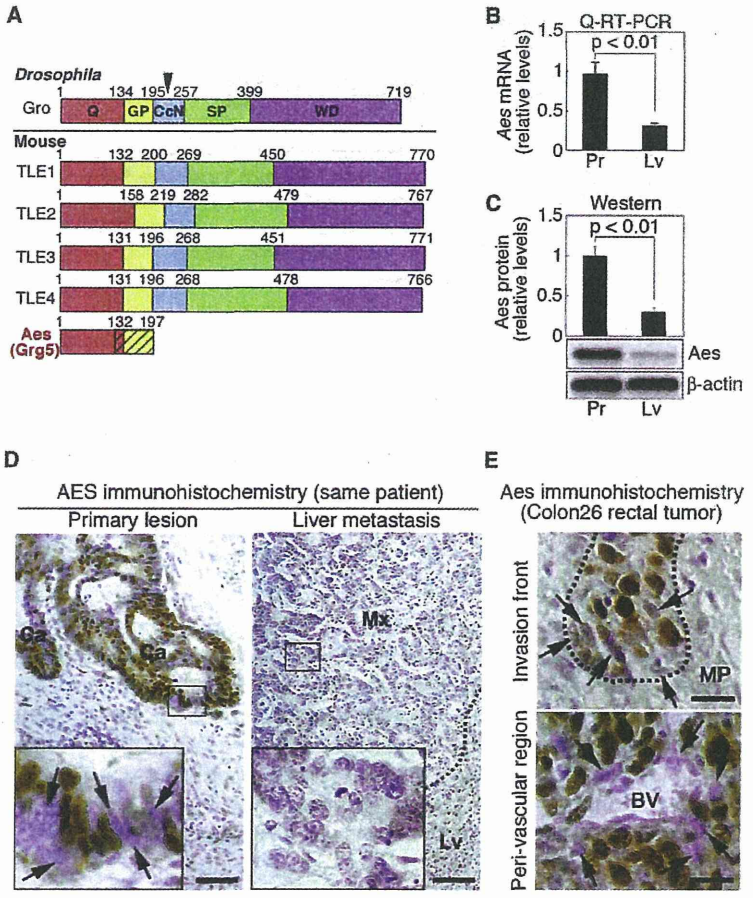

Figure 1. *Aes* as a Metastasis Suppressor Candidate

(A) Schematic representation of fly and mouse Gro/TLE family protein structures. Hatched region in Aes shows a limited identity with TLEs (~65%). Q, glutamine-rich domain (orange); GP, glycine-proline-rich domain (yellow); CcN, domain containing putative phosphorylation sites for cdc2 and casein kinase II (CK2) adjacent to nuclear localization signals (triangle) (blue); SP, serine-proline-rich domain (*green*); WD, domain containing series of tandem repeats of tryptophan and aspartic acid residues (purple). Numbers indicate amino acid residues.

(B) Expression levels of *Aes* mRNA in mouse Colon26 cells determined by quantitative (Q-)RT-PCR. Pr, primary tumors. Lv, liver metastases. Error bars indicate SD. (n = 3).

(C) Expression levels of Aes protein in Colon26 cells determined by western blotting. Same keys as in (B).

(D) Immunostaining for AES in a primary human colon cancer (left) and its liver metastasis (right) from the same patient. Boxed areas are shown in insets, respectively. Dotted line indicates the boundary between metastasis (Mx) and normal liver tissue (Lv). Note that some cancer cells at the invasive fronts had lost expression of *AES* (arrows). Ca, cancer epithelium. Scale bars, 100 μm. Nuclei were counterstained with hematoxylin.

(E) Loss of *Aes* expression on the invasive front of mouse Colon26 primary tumors (arrows). Dotted line indicates the boundary between invading cancer cells and host *muscularis propria* (MP). BV, blood vessel. Scale bars, 10 μm.

See also Figure S1.

1998). Even in such a model, the adenocarcinomas are only locally invasive, and neither intravasation nor distant metastasis is observed during the short life span of these mice. Accordingly, we have screened for candidate genes whose inactivation can stimulate metastasis of transplanted mouse colon cancer cells from the rectum to the liver, the commonest site of metastasis.

RESULTS

Aes as a Metastasis Suppressor Candidate

To identify genes responsible for metastasis suppression, we first prepared a syngeneic and orthotopic transplantation model of colon cancer metastasis in the mouse. When injected into the rectal smooth muscle layer, Colon26 cells can metastasize to the liver, lungs, and lymph nodes in the Balb/c hosts at different efficiencies (Corbett et al., 1975; Kashtan et al., 1992; Tsutsumi et al., 2001) (see Figures S1A–S1F available online). As a preliminary screening, we compared gene expression profiles between the primary tumors and their liver metastases using cDNA microarrays. While many genes showed differential expression, we focused on the category of "transcription regulator activity" in search for master regulators that control metastatic traits. Because cell migration and motility appear to be key traits of metastatic cancer (Christofori, 2006; Weinberg, 2007), we tested ~20 downregulated genes for inhibition of Colon26 invasion in vitro through Matrigel and found one that showed a strong activity, though it was at the 26th of the list (Figure S1G). This gene, *Amino-terminal enhancer of split* (*Aes*), also called *Grg5* in mice, is a member of the *Groucho/Transducin-Like Enhancer of split* (*Gro/TLE*) gene family, with its Q/GP domains showing similarities to those in TLEs (Gasperowicz and Otto, 2005; Lepourcelet and Shivdasani, 2002; Brantjes et al., 2001) (Figure 1A). Although mouse *Aes* helps development of bone and the pituitary gland (Mallo et al., 1995; Brinkmeier et al., 2003), its role in cancer progression has not been investigated. Consistent with the microarray and Matrigel results, mouse *Aes* was significantly downregulated in the liver and lung metastases, upon determinations by quantitative (Q-) RT-PCR (Figure 1B) and western blots (Figure 1C). Importantly, human liver metastatic lesions in 29 out of 52 colon cancer patients (i.e., 56%) expressed significantly lower levels of AES protein than primary tumors from the same patients (Figure 1D). Curiously, some cancer cells had already lost expression of *AES/Aes* at the invasion fronts in both human (Figure 1D, inset in the left panel) and mouse (Figure 1E) colon primary tumors. Furthermore, absence of AES in human colon cancer significantly correlated with vascular invasion ($p < 0.01$), distant metastasis ($p = 0.01$) and progression stages ($p = 0.02$; $n = 83$).

To investigate the roles of *Aes* in colon cancer metastasis, we constructed Colon26 cell derivatives whose *Aes* expression was

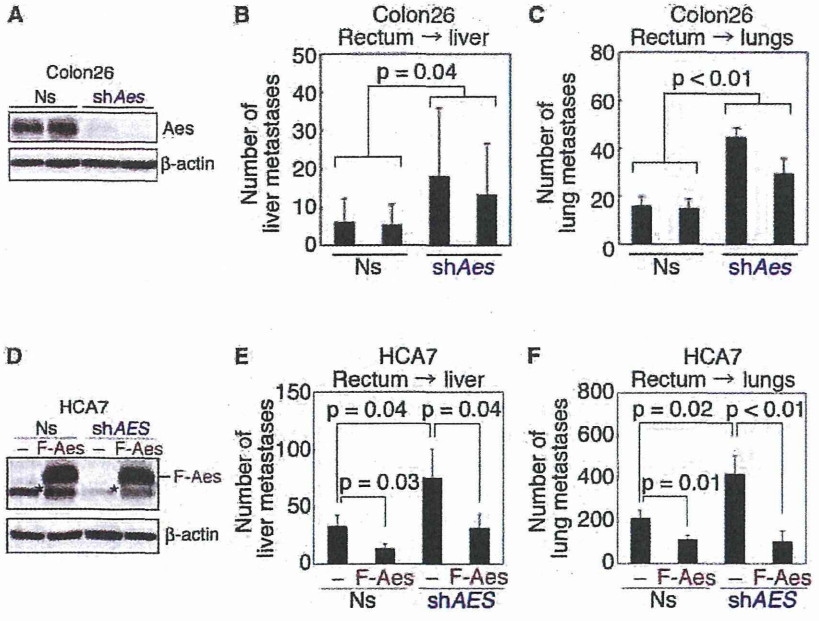

Figure 2. Suppression of Colon Cancer Metastasis by *Aes*

(A–C) Effects of *Aes* knockdown in mouse Colon26 cells (A) on their metastasis to the liver (B) and lungs (C), respectively. Multiple Colon26-derived clonal cell lines were isolated that expressed one of three different shRNA constructs, followed by the rectal transplantation. Data are shown for such cell lines derived from two distinct shRNA clones whose experiments were performed simultaneously, and similar data were obtained with a third clone (not shown). Ns, nonsilencing control. sh*Aes*, shRNA against *Aes* mRNA. Error bars indicate SD (n = 10).

(D–F) Effects of *Aes* overexpression in a human colon cancer cell line HCA7 (D) on its metastasis to nude mouse liver (E) and lungs (F) from the rectum, respectively. A clonal cell line expressing flag-tagged mouse Aes (F-Aes) was compared with a control containing the empty vector (–) (D); left half; Ns for nonsilencing control). The same set of cell lines were introduced with a construct that expressed an shRNA against human *AES* (sh*AES*; (D), right half). Asterisks show the band position for the endogenous human AES protein (western blot analysis). Note that metastasis-promoting effects of sh*AES* was suppressed by overexpression of mouse Aes (F-Aes), excluding the possibility of off-target effects by sh*AES*. Each data set shown is a representative of two. Error bars indicate SD (n = 5).

See also Figure S2.

knocked down constitutively by shRNA constructs (sh*Aes*) (Figure 2A). As anticipated, *Aes* knockdown promoted Colon26 metastasis from the Balb/c mouse rectum to liver (Figure 2B) and lungs (Figure 2C), for all clones derived from three independent shRNAs. Likewise, knockdown of human *AES* (Figure 2D) increased the number of metastases for HCA7 human colon cancer cells (Kirkland, 1985) to both liver (Figure 2E) and lungs (Figure 2F) of nude mice. Convincingly, this knockdown effect was reversed by overexpression of flag-tagged mouse *Aes* (F-Aes) that was not targeted by the shRNA against human *AES* (Figures 2D–2F). We then constitutively overexpressed *Aes* in Colon26 cells at the level five times higher than that of endogenous *Aes*, injected them into the mouse rectum, and found that their metastasis was suppressed significantly to both liver and lungs (Figures S2A–S2D). Notably, *Aes* suppressed lung metastasis of the cancer cells also upon intravenous injections (Figure S2E), another model of hematogenous metastasis that bypasses local invasion and intravasation (Price, 2001). Importantly, neither knockdown nor overexpression of *Aes* affected the size of primary tumors (Figures S2F–S2H). These results indicate that *Aes* suppresses colon cancer metastasis without affecting the growth of primary tumors.

Aes Is an Endogenous Notch Signaling Inhibitor

In colonic tumor formation and its malignant progression, Wnt, TGF-β, Hedgehog, and Notch signaling pathways appear to play key roles (Sancho et al., 2004; van Es et al., 2005; Taketo, 2006; Takaku et al., 1998), not to mention KRAS and p53. Interestingly, Gro/TLE cotranscription factors have been implicated in some of these pathways (Roose et al., 1998; Chen and Courey, 2000; Wang et al., 2002). We first investigated the possible role of Aes in Wnt signaling because of its Q and GP domains similar to those in TLE proteins that can inhibit the signaling (Brantjes et al., 2001). Although we confirmed repression by TLE1 to ~20%, Aes had only marginal effects on LEF1/β-catenin-induced TOPFLASH activation in HEK293 human embryonic kidney cells (Figure S3A). Aes also failed to suppress Wnt signaling in Colon26 cells (Figure S3B, left).

We then assessed the effects of Aes on other signaling pathways in colon cancer cells by transactivation assays using established luciferase reporters. Aes did not affect TGF-β or Hedgehog pathways (Figure S3B, center or right). Instead, Aes significantly inhibited Notch signaling, a critical signaling in development (Artavanis-Tsakonas et al., 1999; Hurlbut et al., 2007; Ilagan and Kopan, 2007), as determined by pGa981-6 reporter containing Rbpj (Recombination signal binding protein of the Jκ immunoglobulin gene, or CSL; CBF1 in human)-binding sites and a luciferase gene (Kato et al., 1997). Namely, expression of exogenously introduced *Aes* dose-dependently repressed both endogenous and RAMIC (Rbpj-associated molecule domain and intracellular domain of the Notch receptor, a recombinant protein equivalent to NICD, Notch intracellular domain) (Kato et al., 1997)-induced transcription of the reporter in Colon26 cells (Figure 3A). Of note, 293T cells showed the strongest activity of endogenous Notch signaling among 30 cell lines analyzed, and Aes caused tighter repression in these cells (to ~20%) (Figure S3C). Consistently, induction of Aes by doxycycline in Colon26 TetONF-Aes cells suppressed expression of endogenous Notch target *Hes1* (Figure S3D). On the other hand, knockdown of *Aes* doubled the activity of both the

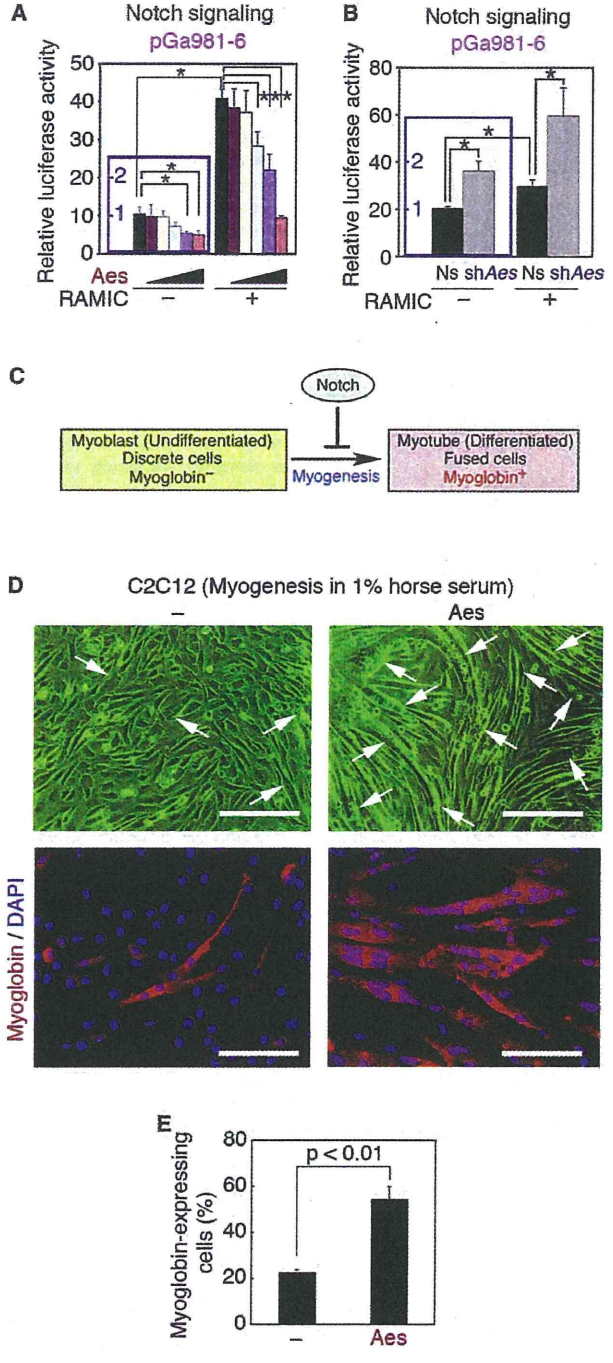

endogenous and RAMIC-induced Notch signaling in Colon26 cells (Figure 3B). Consistent with these data, *Aes* enhanced myogenic differentiation of C2C12 myoblasts in a representative biological assay for Notch signal inhibition (Kato et al., 1997) (Figures 3C–3E).

Because Aes and TLE proteins shared structural similarities (Figure 1A), we next asked whether TLE1 also inhibited Notch signaling. In contrast to Aes, TLE1 failed to repress the RAMIC-induced transactivation in 293T cells, human colon cancer HCT116 cells, and mouse Colon26 cells (Figure 4A; data not shown). Interestingly, however, coexpression with TLE1 significantly potentiated the repression by Aes. It was reported that Aes interacted with TLE1 in yeast (Pinto and Lobe, 1996), and we found coprecipitation of endogenous Aes and TLE1 in the lysates of colonic tumors from $Apc^{\Delta 716}$ mice (Oshima et al., 1995) (Figure 4B). Notably, we found nuclear colocalization of Aes and TLE1 forming distinct foci in $Apc^{\Delta 716}$ adenoma cells (Figure 4C). We further studied subcellular localization of Aes in cultured cells. When transfected alone, Aes fused to *Aequorea coerulescens* GFP (AcGFP-Aes) showed diffuse distribution in both the cytoplasm and nucleoplasm of live HCT116 cells (Figure 4D). Intriguingly, coexpression with TLE1 caused dramatic relocation of AcGFP-Aes to nuclei, causing distinct foci (Figure 4D). Similar results were obtained with 293T and Colon26 cells (data not shown).

We next employed deconvolution microscopy, and analyzed subnuclear localization of the Notch effectors; Rbpj, RAMIC (NICD), and Maml1 (Mastermind-like 1). In the absence of Aes/TLE1 complex, Rbpj, RAMIC, and Maml1 all showed diffuse nucleoplasmic distribution in HCT116 cells. When cotransfected with Aes and TLE1, however, RAMIC and Maml1 relocated to nuclear foci that also contained Aes and TLE1, whereas Rbpj distributed both in the foci and the nucleoplasm (Figures 4E and 4F).

To determine the roles of these nuclear foci in transcription, we performed in situ transcription labeling, and visualized BrUTP incorporation into mRNA during 5 min prior to fixation. When Notch effectors were coexpressed with Aes and TLE1, BrUTP uptake into mRNA was scarce in the nuclear foci where Maml1 resided (Figure 4G). These foci were not stained with anti-PML, anti-SC35, or anti-fibrillarin antibody, suggesting that they are distinct from PML bodies, RNA splicing bodies, and nucleoli (Zimber et al., 2004) (data not shown). Rather, lack of transcription in the foci was reminiscent of Bach2 foci, the nuclear bodies containing HDAC4 (Histone deacetylase 4) and SMRT (Silencing mediator of retinoid and thyroid receptor), and possibly related to matrix-associated deacetylase (MAD) bodies (Downes et al., 2000; Hoshino et al., 2007). In situ nuclear matrix preparation revealed that the Aes nuclear foci were indeed in the insoluble nuclear matrix fraction (Figure 4H). Moreover, HDAC3 was

Figure 3. Inhibition of Notch Signaling by *Aes*

(A and B) Effects of *Aes* overexpression (A) and *Aes* knockdown (B) on Notch signaling in Colon26 cells determined by pGa981-6 luciferase reporter assay in the absence (–) or presence (+) of exogenously introduced RAMIC. Insets (blue frames) show the endogenous reporter activities. Ns, nonsilencing control. *$p < 0.01$ compared with the controls. Error bars indicate SD ($n = 3$).

(C) A schematic representation of the role of Notch signaling in myogenesis.

(D) Effects of Aes on myoblast differentiation. Rat C2C12 myoblasts were transfected with either the vector or Aes cDNA, and three stable clones were isolated, respectively. Myogenesis was induced by a medium containing 1% horse serum for 4 days. Myoglobin, a myotube marker, was immunostained (red) in C2C12 clones with or without overexpressed Aes. Nuclear DNA was stained with DAPI (blue). Arrows, myotubes with multiple nuclei. Scale bars, 100 μm.

(E) Quantification of the myoglobin-expressing cells in (D). Error bars indicate SD ($n = 3$).

See also Figure S3.